

Optical phonons in $\text{YBa}_2\text{Cu}_4\text{O}_8$ and $\text{Y}_2\text{Ba}_4\text{Cu}_7\text{O}_{15-\delta}$

E. T. Heyen, R. Liu, C. Thomsen, R. Kremer, and M. Cardona
*Max-Planck-Institut für Festkörperforschung, Heisenbergstrasse 1,
 D-7000 Stuttgart 80, Federal Republic of Germany*

J. Karpinski, E. Kaldis, and S. Rusiecki
Laboratorium für Festkörperphysik, Eidgenössische Technische Hochschule, 8093 Zürich, Switzerland
 (Received 26 January 1990)

We present Raman spectra of high-temperature superconducting single crystals of $\text{YBa}_2\text{Cu}_4\text{O}_8$ and $\text{Y}_2\text{Ba}_4\text{Cu}_7\text{O}_{15-\delta}$, differing from the well-known $\text{YBa}_2\text{Cu}_3\text{O}_{7-\delta}$ by having double CuO chains. By performing polarization-dependent measurements, we were able to identify the symmetry of the observed phonons. In both materials, we detected four out of six Raman-allowed modes of the double Cu(1)-O(1) chains and assign the peaks to Cu(1) A_g (250 cm^{-1}), O(1) A_g (605 cm^{-1}), Cu(1) B_{3g} (314 cm^{-1}), and O(1) B_{2g} (228 cm^{-1}) in addition to the 5 A_g phonons (in $\text{YBa}_2\text{Cu}_4\text{O}_8$ near 104, 153, 341, 438, and 500 cm^{-1}), which are also present in the well-known $\text{YBa}_2\text{Cu}_3\text{O}_{7-\delta}$. Contrary to previous reports of Raman scattering on double-CuO₂-plane superconductors, B_{2g} and B_{3g} phonons can unambiguously be observed. They are, in fact, stronger than some of the A_g phonons. The peaks at 605, 314, 250, and 228 cm^{-1} are more than twice as large in $\text{YBa}_2\text{Cu}_4\text{O}_8$ than in $\text{Y}_2\text{Ba}_4\text{Cu}_7\text{O}_{15-\delta}$, thus confirming that they are chain related. The Raman intensities of the A_g modes at 250, 500, and 605 cm^{-1} are much larger in yy (along the chains) than in xx polarization, proving that the crystals are untwinned and stressing the importance of the chains for the Raman activity of these modes. When lowering the temperature below $T_c=74\text{ K}$ the B_{1g} -like O(2)-O(3) phonon near 104 cm^{-1} as well as the Ba A_g phonon at 341 cm^{-1} exhibit a rather sharp softening. The Ba mode shows a pronounced Fano line asymmetry, while that of the O(2)-O(3) line is rather weak.

I. INTRODUCTION

In the past, Raman scattering has successfully been used in high- T_c superconductors, not only to detect and assign optical phonons,^{1,2} but also to prove the existence of strong electron-phonon coupling,^{3,4} to measure the opening of a superconducting gap,^{3,5,6} to find x - y anisotropic properties in these orthorhombic compounds,³ and to determine the oxygen content in $\text{YBa}_2\text{Cu}_3\text{O}_{7-\delta}$.⁷⁻⁹ Using resonant Raman scattering, energy and location of electronic resonances and their coupling to optical phonons have recently been investigated.^{10,11} Also excitations of the Cu spin system have been examined.¹²

Unfortunately, the vibrations involving the Cu-O chains in $\text{YBa}_2\text{Cu}_3\text{O}_{7-\delta}$ (Y-Ba-Cu-O 1:2:3) cannot be observed by Raman scattering since they have odd parity and are therefore only infrared-active. These restrictions are not valid anymore for the 80-K superconductor $\text{YBa}_2\text{Cu}_4\text{O}_8$ (Y-Ba-Cu-O 1:2:4),^{13,14} differing from $\text{YBa}_2\text{Cu}_3\text{O}_7$ in that the single Cu-O chain has been replaced by a double Cu-O chain with edge-sharing, square-planar oxygen coordination¹⁵ (Figs. 1 and 2). Thus the chain vibrations become Raman active. For the same reasons, chain phonons can also be detected in $\text{Y}_2\text{Ba}_4\text{Cu}_7\text{O}_{15-\delta}$ (Y-Ba-Cu-O 2:4:7),^{17,18} consisting of alternately stacked Y-Ba-Cu-O 1:2:3 and Y-Ba-Cu-O

1:2:4 units. Recently, Krantz *et al.*¹⁹ reported preliminary Raman results on crystallites found in ceramic samples. They found peaks near 252 and 602 cm^{-1} which they assigned as A_g symmetry modes of Cu(1) and O(1).

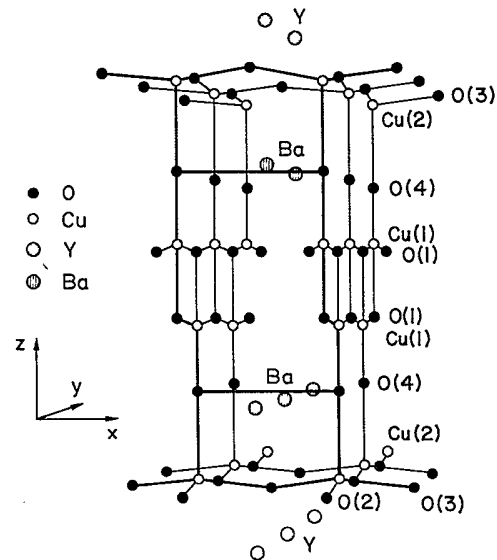


FIG. 1. Crystal structure of Y-Ba-Cu-O 1:2:4. (Modified version of the figure in Ref. 16.)

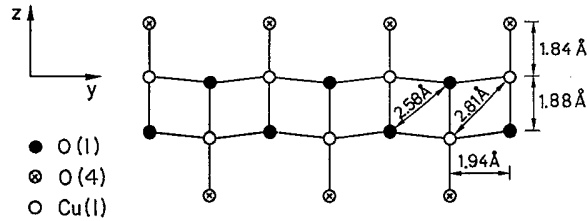


FIG. 2. Double Cu(1)-O(1) chain network with neighboring O(4) atoms in the y - z plane of Y-Ba-Cu-O 1:2:4.

Using Raman spectroscopy on untwinned Y-Ba-Cu-O 1:2:4 and Y-Ba-Cu-O 2:4:7 crystals we detected four of the six possible phonons involving chain motion. By studying the polarization properties, we were able to assign the observed features. In particular, we identified strong B_{2g} and B_{3g} symmetry modes involving the motion of the O(1) and Cu(1) atoms along the a and b axes, respectively. B_{2g} or B_{3g} modes have generally not been convincingly observed in any high- T_c compound with a double CuO_2 plane per unit cell.²⁰

Furthermore, we found that the Ba A_g phonon near 104 cm^{-1} as well as the B_{1g} -like O(2)-O(3) mode at 341 cm^{-1} exhibit a sharp softening when the sample is cooled below T_c . Also the intensity of the Ba mode decreases by a factor of 5 when cooling from room temperature to T_c and then remains almost constant. These results will be published elsewhere.²¹

This paper is organized as follows: In Sec. II, we describe the growth and structure of Y-Ba-Cu-O 1:2:4 and Y-Ba-Cu-O 2:4:7 untwinned single crystals. Based on the factor group analysis we discuss in Sec. III the Raman-active vibrations that might be observed in certain scattering geometries. We then present in Secs. IV and V Raman spectra taken on Y-Ba-Cu-O 1:2:4 and Y-Ba-Cu-O 2:4:7, respectively, in 11 different polarization configurations each. In Sec. VI we discuss results using the polarization properties, we determine the symmetry of the observed phonons and assign them to vibrations of certain atoms. In addition, we are able to demonstrate by Raman scattering that the crystals are untwinned and determine some a - b -anisotropy properties.

II. STRUCTURE AND GROWTH OF $\text{YBa}_2\text{Cu}_4\text{O}_8$ AND $\text{Y}_2\text{Ba}_4\text{Cu}_7\text{O}_{15-\delta}$

The structure of Y-Ba-Cu-O 1:2:4 (space group $Ammm$) has been derived by x-ray diffraction for two-phase thin films¹⁵ and refined in pure bulk samples¹³ with neutron diffraction.^{22,23} It is similar to that of Y-Ba-Cu-O 1:2:3 except for the double chains. These introduce a shift of $b/2$ parallel to the b axis between two subsequently stacked Y-Ba-Cu-O 1:2:3 blocks leading to a doubling of the unit cell in c direction. The structure is shown in Figs. 1 and 2. To conform with the Raman literature on Y-Ba-Cu-O 1:2:3, we call O(1) the equatorial oxygen in the Cu(1)-O chains, and O(4) the apical oxy-

gen of the Cu(2)-O pyramids which is bridging the chains and the planes. This is different from the convention used in Refs. 13-18 and 22-34. The lattice constants of stoichiometric polycrystalline material were determined by x rays (Guinier camera, and internal Si-standard according to the National Institute of Standards and Technology) to be $a=3.8415(3)\text{ \AA}$, $b=3.8708(5)\text{ \AA}$, and $c=27.240(2)\text{ \AA}$.²²

Small single crystals of Y-Ba-Cu-O 1:2:4 were grown at high oxygen pressure (590 bars, $T_{\text{max}}=1140^\circ\text{C}$) in a BaO-CaO rich flux.²⁴ Although crystals up to 5 mm are formed in the flux, only pieces up to 1.5-2 mm can be mechanically separated from the solidified molten solution. The high-pressure phase diagram of Y-Ba-Cu-O 1:2:4 and Y-Ba-Cu-O 2:4:7 (Ref. 25) shows that the first crystals to appear during solidification are those of Y-Ba-Cu-O 2:4:7, at least for oxygen pressures $P \leq 2900$ bars. It is not known how the phase diagram changes in the presence of the flux. However, if we assume a more or less constant shift of the phase boundaries, we can understand why in the same batch both Y-Ba-Cu-O 2:4:7 and Y-Ba-Cu-O 1:2:4 crystals appear. Further support for this assumption is the occasional appearance of overgrowths of Y-Ba-Cu-O 1:2:4 on Y-Ba-Cu-O 2:4:7, i.e., crystal platelets nucleated as Y-Ba-Cu-O 2:4:7, have overgrowths of Y-Ba-Cu-O 1:2:4 in the last stage of growth. The crystallographic characterization in order to select perfect crystals from a growth batch, like those used for the electron density measurements,²⁶ is quite time consuming.

The lattice constants of the Y-Ba-Cu-O 1:2:4 untwinned single crystal used in this work were determined with an x-ray diffractometer to be $a=3.852\text{ \AA}$, $b=3.879\text{ \AA}$, and $c=27.27\text{ \AA}$. This slight systematic increase, as compared with the stoichiometric polycrystalline material, is mainly due to the lack of internal standardization in the single-crystal work. Meissner effect measurements show a rather sharp superconducting transition at 74 K. Due to the narrow homogeneity range of Y-Ba-Cu-O 1:2:4,²⁴ the oxygen content does not greatly vary in Y-Ba-Cu-O 1:2:4 samples.

The opposite is true for the grossly nonstoichiometric compound Y-Ba-Cu-O 2:4:7. Its structure is formed from alternating blocks of 1:2:3 and 1:2:4, i.e., it contains both single and double chains so that four blocks have to be accommodated in the unit cell and the c axis becomes very long. This compound was discovered with electron diffraction in solidified high-temperature solutions of Y-Ba-Cu-O 1:2:3 under high oxygen pressure²⁷ and its structure has been determined on single crystals.¹⁷ Recently, it was shown that the oxygen content can be varied in a wide range $-0.02 \leq \delta \leq 0.70$, leading to changes of T_c between 16 and 70 K.²⁸ Large variations appear also for the lattice constants; the a and c axes elongate and the b axis contracts with decreasing oxygen content. The lattice constants of the untwinned crystal investigated in this work were found with the diffractometer to be $a=3.861\text{ \AA}$, $b=3.881\text{ \AA}$, and $c=50.45\text{ \AA}$, which gives an orthorhombicity $(b-a)/(b+a)$ of 2.58×10^{-3} , as com-

pared with 3.0×10^{-3} found earlier for the stoichiometry $Y_2Ba_4Cu_7O_{14.4}$.²⁸ As the dependence of the orthorhombicity on the oxygen stoichiometry is known,²⁸ we can roughly estimate the oxygen content of the crystal to be $\cong 14.3 - 14.4$, i.e., rather low.

The existence of the double chains stabilizes the oxygen in Y-Ba-Cu-O 1:2:4 up to 850°C, preventing the appearance of a phase transition, as in Y-Ba-Cu-O 1:2:3. Therefore, no reason for massive twinning exists and the crystals are twin free.²³ Also the Y-Ba-Cu-O 2:4:7 does not show twinning.²⁹ Despite its large homogeneity range, no phase transition to a tetragonal phase takes place, because the stable double chains prevent its formation. Both, the x-ray structural analysis on a single Y-Ba-Cu-O 2:4:7 crystal¹⁷ and ongoing neutron diffraction as a function of nonstoichiometry,³⁰ show that a certain percentage of the single chains is parallel to the *a* axis, i.e., perpendicular to the double chains. This percentage is for a stoichiometric sample roughly 30% and increases as the concentration of the single chains decreases with decreasing oxygen content. It would be interesting to trace these misoriented single chains by Raman spectroscopy.

In a recent review,³¹ the structural anomalies introduced by the double chains are discussed in detail. Here, we just want to mention that due to the combination of the increased coordination of oxygen and the rather short Cu(1)-O(4) bond length (1.841 Å), compared to SrCuO₂ (1.91 Å), the chains parallel to the *b* axis becomes more rigid and the following anomalies appear in Y-Ba-Cu-O 1:2:4:

(a) The thermal expansion of the lattice constant *b*, which contains the double chains, is anomalous:²³ in the superconducting state, *b* does not contract when cooling, opposite to the *a* and *c*.

(b) Also the compressibility of *b* at room temperature is anomalous.³² The value of the linear compressibility in the direction of the *b* axis is 1.0×10^{-3} /GPa as compared to the very high compressibilities in the *a* (2.8×10^{-3}) and *c* axes (4.5×10^{-3}). The bulk moduli $B=112$ GPa at 301 K and 122 GPa at 30 K are very low as compared with other high-*T_c* superconductors, e.g., ≈ 180 for $La_{1-x}Sr_xCuO_{4-x}$ and $YBa_2Cu_3O_{7-x}$ according to Ref. 33.

(c) Another interesting aspect of these compounds is the increased anisotropy in the *a-b* plane and along the *c* axis due to the double chains. Electrical and magneto-optical measurements³⁴ show a large anisotropy between the *b* axis which contains the double chains and the *a* axis which does not contain any chains in the Y-Ba-Cu-O 1:2:4 or only 30% of the single chains in Y-Ba-Cu-O 2:4:7.

III. VIBRATIONAL ANALYSIS

In Y-Ba-Cu-O 1:2:3, the CuO chains are contributing $2(B_{1u}+B_{2u}+B_{3u})$ infrared-active optical phonons while vibrations of the other atoms in the unit cell involve $5(A_g+B_{2g}+B_{3g})$ Raman-active and $5(B_{1u}+B_{2u}+B_{3u})$ infrared-active phonons.² The A_g Raman modes involv-

ing an even-parity motion in the *c* direction have been unambiguously observed near 120, 154, 335, 435, and 500 cm^{-1} and were assigned to the vibrations of Ba, Cu(2), O(3)-O(2) out-of-phase, O(3)-O(2) in-phase, and O(4), respectively. Among the infrared-active phonons, only 5 B_{1u} modes have been clearly identified near 155 (Ba), 191 (Y), 275 [O(2)-O(3) out-of-phase], 310 [O(2)-O(3) in-phase], and 570 cm^{-1} [O(4)].³⁵

When, as in Y-Ba-Cu-O 1:2:4, an additional CuO chain is introduced, the space group changes from *Pmmm* to *Ammm* while the point group remains *mmm* (D_{2h}). Now the Cu(1) and O(1) atoms are no longer in the center of inversion and their site symmetry changes from D_{2h} to C_{2v}^2 ; they therefore contribute $2(A_g+B_{2g}+B_{3g}+B_{1u}+B_{2u}+B_{3u})$ optical phonons instead of $2(B_{1u}+B_{2u}+B_{3u})$.³⁶ An analysis of the symmetry coordinates shows that the A_g , B_{2g} , and B_{3g} modes correspond to vibrations along the *c*, *a*, and *b* axes, respectively.

Y-Ba-Cu-O 2:4:7 has alternatingly one single chain similar to Y-Ba-Cu-O 1:2:4 and double chains like in Y-Ba-Cu-O 1:2:3. Its space group remains *A*-centered orthorhombic *Ammm*, but the primitive cell now contains 28 atoms. A simple group-theoretical analysis yields $12(A_g+B_{2g}+B_{3g})+15(B_{1u}+B_{2u}+B_{3u})$ optical phonons in Y-Ba-Cu-O 2:4:7. This effectively means that all *Z* points of the corresponding infrared-active branches in Y-Ba-Cu-O 1:2:3 now also become Raman-active modes at the Y-Ba-Cu-O 2:4:7 Γ point; in other words, the Brillouin zone is folded in Γ -*Z* direction. We know well from lattice-dynamical calculations³⁷ and also from linear muffin-tin orbital (LMTO) band structure calculations³⁸ that there hardly exists any dispersion in the *z* direction of the phonon or electron bands showing that there is very little long-range coupling between Y-Ba-Cu-O 1:2:3-like primitive cells in that direction. Therefore, the folded modes will have nearly the same frequency as those at the original zone center and, anyhow, be only very weakly Raman active. Thus, the set of phonon energies seen in Raman spectra should be the same for Y-Ba-Cu-O 1:2:4 as for Y-Ba-Cu-O 2:4:7. There just remains a difference in the intensities of the chain-related Raman modes. Since the density of double chains in Y-Ba-Cu-O 1:2:4 is roughly twice as large as in Y-Ba-Cu-O 2:4:7, we expect the chain Raman modes which originate only in double chains to be twice as intense in Y-Ba-Cu-O 1:2:4 as in Y-Ba-Cu-O 2:4:7.

Which phonon frequencies might be expected? Most atomic distances of Y-Ba-Cu-O 1:2:4 [$a=3.852$ Å, $b=3.879$ Å, Cu(2)-O(4)=2.288 Å, Cu(1)-O(4)=1.841 Å (Ref. 26)] and Y-Ba-Cu-O 2:4:7 [$a=3.861$ Å, $b=3.881$ Å, Cu(2)-O(4)=2.28 Å, Cu(1)-O(4)=1.83 Å (Ref. 17)] do hardly change with respect to Y-Ba-Cu-O 1:2:3 [$a=3.822$ Å, $b=3.891$ Å, Cu(2)-O(4)=2.30 Å, Cu(1)-O(4)=1.85 Å (Ref. 39)]. Thus we expect the frequencies of the modes of Cu(2) (154 cm^{-1}), O(2)-O(3) (335 and 435 cm^{-1}) not to differ much from those in Y-Ba-Cu-O 1:2:3. For even, Raman-active vibrations, the Cu(1) atom is no longer at rest so that the O(4) (500 cm^{-1}) and Ba (120

cm^{-1}) phonons might soften slightly, depending on the rigidity of the two-dimensional O(4)-Cu(1)-O(1) network (Fig. 2).

Let us now consider the A_g modes of the O(1) and Cu(1) atoms along the z axis. Since the masses of copper and oxygen atoms are quite different, we expect the O(1), O(4), and Cu(1) vibrations not to couple strongly. The O(1) atom induces a stretching of the quite short (1.88 Å) Cu(1)—O(1) bond. In addition the O(1) feels the strong Coulomb forces of the neighboring Cu(1) (1.94 Å), the other O(1) (2.58 Å) and O(4) atoms (2.78 Å). We therefore expect the O(1) A_g frequency to be higher than that of O(4) A_g near 500 cm^{-1} which depends only on the Cu(1)-O(4) (1.84 Å) and O(1)-O(4) (2.78 Å) stretching.

Similarly, we argue that the Cu(1) A_g frequency should be higher than that of the Cu(2)- A_g motion (near 154 cm^{-1} in Y-Ba-Cu-O 1:2:3). While the Cu(2) mode depends mainly on the stretching of the long and therefore weak Cu(2)—O(4) bond (2.29 Å) and the bending of the Cu(2)—O(2)—O(3) bonds ($\sim 1.94 \text{ Å}$), the Cu(1) is located within only 1.84 Å and 1.88 Å from the O(4) and O(1) atoms, respectively, yielding strong stretching forces. In addition it feels the O(1)—Cu(1) bonding and the strong Cu(1)-Cu(1) repulsion which might lead to the observed dimpling of the double chains (Figs. 1 and 2). We should mention here that the Coulomb force constant for a stretching motion of an ion located centrally between two oppositely charged ions is only twice as large as that for the corresponding bending, while the force constant depends on the third power of the atomic distances. Therefore the Cu(1) mode will be substantially higher than the Cu(2) A_g mode.

We now discuss the B_{3g} and B_{2g} vibrations along the y and x axis, respectively. The environment for the O(4) atom is practically unchanged with respect to Y-Ba-Cu-O 1:2:3, therefore the O(4) B_{3g} and B_{2g} frequencies should remain essentially the same. Unfortunately, those modes, for unknown reasons, are too weak to be easily detected, so they should hardly be seen in Y-Ba-Cu-O 1:2:4. [In particular, the O(4) B_{3g} line should not vanish since its intensity depends mainly on the O(4)—O(1) bond and should be proportional to $(\alpha'_{\parallel} - \alpha'_{\perp})^2$, where α'_{\parallel} and α'_{\perp} are the derivatives of the longitudinal and transverse polarizabilities of the O(4)—O(1) bond with respect to its length.] The Cu(1) B_{3g} vibration along the y axis will have a relatively high frequency since it is located in a quite rigid square Cu(1)-O(1) environment with two other Cu(1) atoms within a distance of 2.81 Å. Since the conditions are similar to the Cu(1) A_g vibration parallel to the z axis discussed above they should have a comparable phonon frequency. The motion of the O(1) atom in y direction might correspond to the highest observed phonon frequency. The Cu(1)—O(1) bonds involved in this mode (1.94 Å) are slightly longer than those for the O(1) A_g mode (1.88 Å), but in the first case there are two such bonds whereas in the latter there is only one. The fourfold oxygen coordination (Fig. 2) is similar for both modes, they might thus both have a

frequency around 600 cm^{-1} .

Both B_{2g} symmetry vibrations of O(1) and Cu(1) along the x axis will be very low in energy, since they are just bending modes if we neglect the interaction with the Ba atom which is quite far away [Ba-O(1)=2.97 Å, Ba-Cu(1)=3.44 Å]. The corresponding chain-bending modes in Y-Ba-Cu-O 1:2:3 were calculated by Kress *et al.*³⁷ to be near 165 and 80 cm^{-1} for O(1) and Cu(1), respectively. Since the double chains are probably quite rigid, these frequencies should be somewhat higher in Y-Ba-Cu-O 1:2:4.

IV. RESULTS ON Y-Ba-Cu-O 1:2:4

We obtained Raman spectra of Y-Ba-Cu-O 1:2:4 twinned single crystals using a micro-Raman setup together with a SPEX Industries triple spectrometer and a multichannel detection system. As excitation source we used the 4765-Å line of an Ar⁺ ion laser. The power was kept below 5 mW. Since considerable amounts of reflected light are unfortunately collected in our micro-Raman setup, we could not measure Raman shifts below 140 cm^{-1} . We therefore also took a Raman spectrum with a regular "macro" setup which works down to about 70 cm^{-1} . After checking the orientation of the axes with x rays, the samples were aligned in such a way that its a , b , and c axes correspond to the x - y - z laboratory system, respectively.

Raman spectra of Y-Ba-Cu-O 1:2:4 in all possible polarization configurations are shown in Figs. 3, 4, and 5

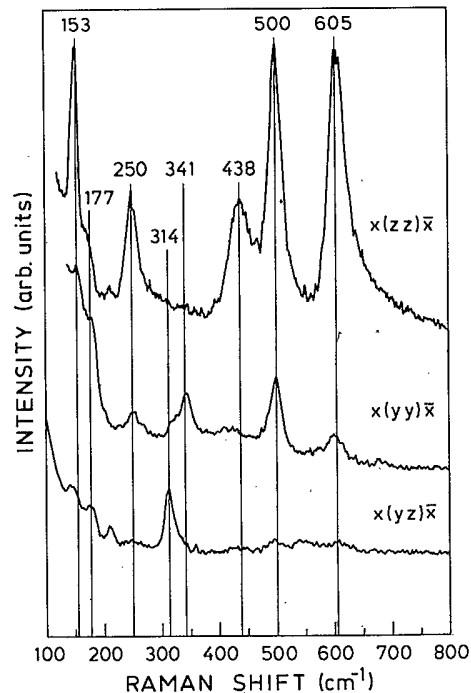


FIG. 3. Polarized Raman spectra of Y-Ba-Cu-O 1:2:4 with the incident light along the x axis taken at 295 K with a micro-Raman setup.

for the laser beam hitting the sample along the x , y , and z axes, respectively. The polarizations are labeled with the Porto notation $i(jk)l$, where i and l refer to the direction of propagation and j and k to the direction of the electrical-field vectors of incident and scattered light, respectively. The x' and y' directions are rotated by 45° with respect to the x and y axes around the z axis. Spectra taken on different spots of the sample all look very similar. There are six peaks at 153, 250, 341, 438, 500, and 605 cm^{-1} appearing only in the spectra where the polarizations of incident and scattered light are along xx , yy , $x'x'$, $x'y'$, and zz , but not in yz , xz , or xy configurations (except some very weak structures that seem due to polarization leakage). These peaks correspond therefore to A_g phonons.

The mode near 341 cm^{-1} exhibits a near- B_{1g} symmetry in the D_{4h} -tetragonal approximation, as is shown by the fact that this peak is observed in xx , yy , $x'y'$ polarizations, but not in $x'x'$ and zz . There still is some leakage in the xy and $x'x'$ spectra, probably due to a small misalignment of the crystal which was not rectangular.

Note that the A_g phonons at 250, 500 and 605 cm^{-1} that are mainly zz polarized appear also strongly in yy configuration, but not in xx . The 500-cm^{-1} mode is in yy polarization even stronger than the 341-cm^{-1} peak that usually dominates in Y-Ba-Cu-O 1:2:3. This x - y anisotropy proves that the crystal is untwinned. Note that in Y-Ba-Cu-O 1:2:3 the 500-cm^{-1} peak is in yy polarization also stronger than in xx (Ref. 3) but the difference is not as large as for the 1:2:4 compound. This result is expected when one considers that the anisotropy is produced by the chains. It can also be seen that the 153-cm^{-1} line is strongest in zz polarization, absent in the $y(xx)\bar{y}$ and $z(xx)\bar{z}$ but visible in the $x(yy)\bar{x}$ and $z(yy)\bar{z}$ configuration, yielding also x - y anisotropy for this mode.

The $x(yz)\bar{x}$ and $y(xz)\bar{y}$ spectra clearly show peaks at 314 and 228 cm^{-1} that are not present in other spectra and are therefore of B_{3g} and B_{2g} symmetry, respectively. Contrary to Y-Ba-Cu-O 1:2:3 where B_{2g} and B_{3g} modes appear, if at all, extremely weakly,²⁰ we stress that here these peaks have a considerable strength; the 314-cm^{-1} phonon is stronger than the B_{1g} phonon at 341 cm^{-1} .

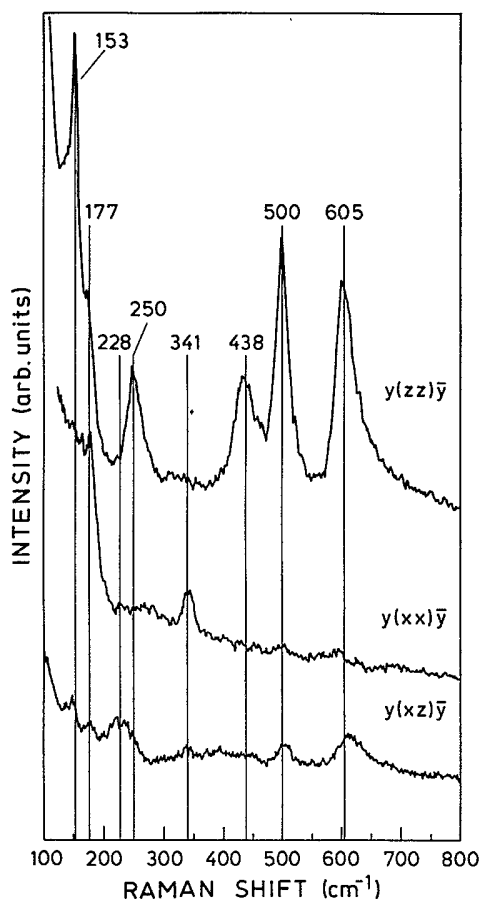


FIG. 4. Polarized Raman spectra of Y-Ba-Cu-O 1:2:4 with the incident light along the y axis taken at 295 K with a micro-Raman setup.

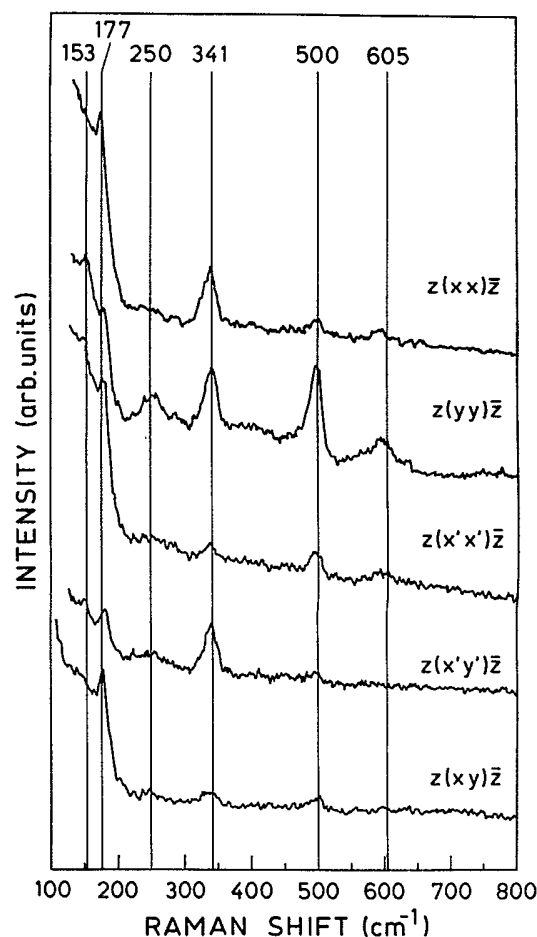


FIG. 5. Polarized Raman spectra of Y-Ba-Cu-O 1:2:4 with the incident light along the z axis taken at 295 K with a micro-Raman setup.

The $y(xz)\bar{y}$ spectrum shows another very weak feature near 400 cm^{-1} that might also exist as a shoulder in the $y(zx)\bar{y}$ spectra and another peak near 140 cm^{-1} whose presence in other geometries could not be checked due to strong Rayleigh scattering. In addition, a feature at 140 cm^{-1} is also observed in the $x(yz)\bar{x}$ spectrum. From the spectra in Fig. 4 it cannot therefore be proven unambiguously whether those peaks have B_{2g} symmetry. The $y(xz)\bar{y}$ spectrum also exhibits a peak at 610 cm^{-1} . One might think that this is just due to polarization leakage of the strong 605 cm^{-1} A_g mode seen in $y(zx)\bar{y}$ configuration. But then we would expect the 500 cm^{-1} A_g mode to exhibit a similar leakage, which is not observed. Furthermore, a leakage feature should also be centered at 605 cm^{-1} .

A rather strong peak which does not show any polarization dependence and whose strength varies from spot to spot appears in all spectra at 177 cm^{-1} . It is therefore definitely not an intrinsic feature of the Y-Ba-Cu-O 1:2:4 structure, but probably related to oxygen disorder or an impurity mode of unknown origin. Similarly, we sometimes observed another small peak near 215 cm^{-1} , also probably due to defects.

In order to see low-frequency phonons, we also took a spectrum with a macroscopic setup where the laser beam was focused with a 6-cm lens onto the a - b plane of the sample in a 70° scattering configuration. We then have a high rejection of the reflected laser beam and can, consequently, measure down to 70 cm^{-1} . The spectrum taken without analyzer is displayed in Fig. 6. In addition to the features already shown in Fig. 5 we see another peak at 104 cm^{-1} , close to the position where the Ba mode of Y-Ba-Cu-O 1:2:3 is usually observed.² This peak exhibits a strongly asymmetric Fano line shape, whereas the asymmetry of the B_{1g} -like peak near 341 cm^{-1} is extremely small. In Y-Ba-Cu-O 1:2:3, the Fano line shape of the latter mode is an important indication of the strong cou-

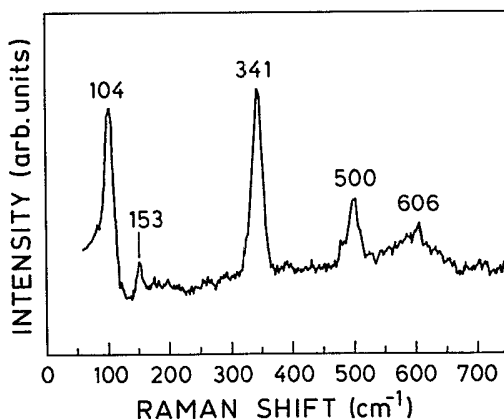


FIG. 6. Unpolarized Raman spectrum of Y-Ba-Cu-O 1:2:4 with the incident light along the z axis taken at 295 K with a macro-Raman setup.

pling of this phonon to electronic transitions in the CuO_2 planes.⁴⁰ The Fano line shape also leads to a shifted peak maximum. While the maximum appears at 104 cm^{-1} the intrinsic phonon frequency is higher, possibly as much as 10 cm^{-1} . We have not attempted to fit the line shape in order to get the intrinsic parameters.

When lowering the temperature, the Ba A_g as well as the O(2)-O(3) B_{1g} -like phonons exhibit a sharp softening at T_c . This observation is different from those on Y-Ba-Cu-O 1:2:3, where only the O(2)-O(3) mode softens, and challenges the current point of view about the coupling between Ba and the superconducting carriers. These two phonons also show a Fano line shape. We have also observed the existence of a temperature-independent background, but not an opening of a superconducting gap. These results will be published elsewhere.²¹

V. RESULTS ON Y-Ba-Cu-O 2:4:7

Spectra taken on Y-Ba-Cu-O 2:4:7 with a micro-Raman setup under similar conditions as for Y-Ba-Cu-O 1:2:4 are shown in Figs. 7–9. Note that contrary to the Y-Ba-Cu-O 1:2:4 spectra, the xx/yy and xz/yz spectra in Figs. 7 and 8 have been magnified by factors of 3 and 5, respectively. With the exception of strong changes in amplitude, these spectra look very similar to those of Y-Ba-Cu-O 1:2:4. Polarization selection rules and frequencies remain nearly the same: We observe A_g modes at 147, 250, 448, 500, and 606 cm^{-1} , a B_{1g} (D_{4h} symmetry)-like

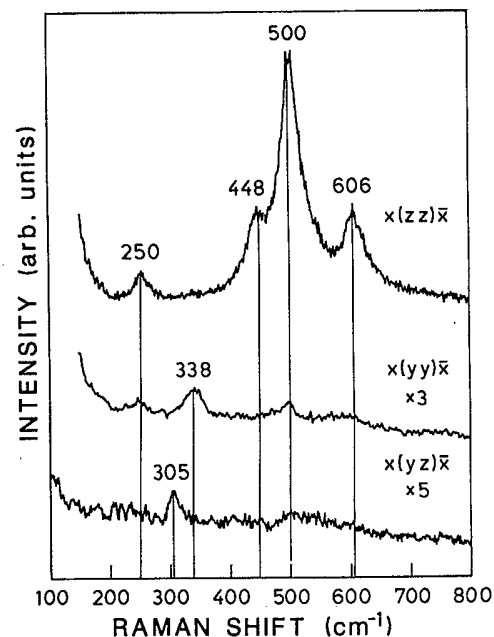


FIG. 7. Polarized Raman spectra of Y-Ba-Cu-O 2:4:7 with the incident light along the x axis taken at 295 K with a micro-Raman setup. yy and yz spectra have been magnified by a factor of 3 and 5, respectively.

A_g line near 338 cm^{-1} , a B_{3g} peak at 305 cm^{-1} , and a B_{2g} mode around 236 cm^{-1} .

Four major differences appear between Y-Ba-Cu-O 1:2:4 and Y-Ba-Cu-O 2:4:7 spectra:

(i) The 250- and 605-cm^{-1} peaks are in Y-Ba-Cu-O 1:2:4 about twice as large as in Y-Ba-Cu-O 2:4:7 with respect to the other peaks. Also the B_{2g} and B_{3g} peaks appear much stronger, e.g., in comparison to the B_{1g} -like peak.

(ii) The a - b anisotropy is particularly striking in Y-Ba-Cu-O 1:2:4, much larger than in Y-Ba-Cu-O 2:4:7 or Y-Ba-Cu-O 1:2:3,³ as demonstrated by the difference in Raman amplitudes (e.g., the 500-cm^{-1} mode) between the xx and yy spectra. Furthermore, the 147-cm^{-1} peak does not show an a - b anisotropy, as demonstrated by nearly equal intensities in the $z(xx)\bar{z}$ and $z(yy)\bar{z}$ spectra. This behavior is very different from that in Y-Ba-Cu-O 1:2:4 (discussed in Sec. IV), but similar to Y-Ba-Cu-O 1:2:3.³

(iii) The zz amplitudes appear to be about 3–4 times larger in Y-Ba-Cu-O 2:4:7 (in this respect similar to Y-Ba-Cu-O 1:2:3) than in Y-Ba-Cu-O 1:2:4 with respect to the observed xx or yy amplitudes, indicating that the c - a/b anisotropy (e.g., in the absorption) is larger in Y-Ba-Cu-O 2:4:7 (or Y-Ba-Cu-O 1:2:3) than in Y-Ba-Cu-O 1:2:4. Since the surface qualities on both samples were different, we have to bear in mind that this anisotropy property may not be intrinsic.

(iv) While the oxygen modes of the CuO_2 planes in

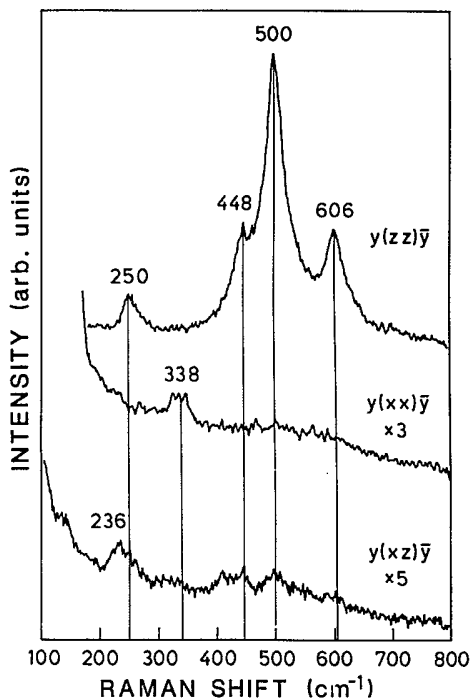


FIG. 8. Polarized Raman spectra of Y-Ba-Cu-O 2:4:7 with the incident light along the y axis taken at 295 K with a micro-Raman setup. xx and xz spectra have been magnified by a factor of 3 and 5, respectively.

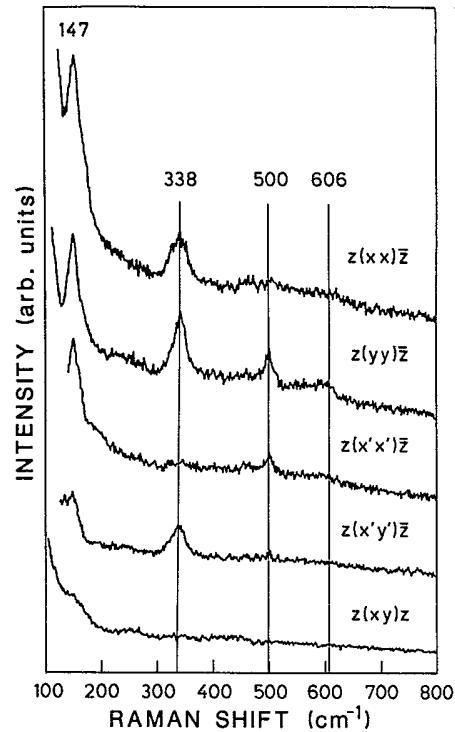


FIG. 9. Polarized Raman spectra of Y-Ba-Cu-O 2:4:7 with the incident light along the z axis taken at 295 K with a micro-Raman setup.

Y-Ba-Cu-O 1:2:4 have similar frequencies (341 and 438 cm^{-1}) as in Y-Ba-Cu-O 1:2:3, the corresponding phonons in Y-Ba-Cu-O 2:4:7 are somewhat further apart, near 338 and 448 cm^{-1} . Also the B_{2g} and B_{3g} modes are clearly shifted. In Y-Ba-Cu-O 1:2:4 or Y-Ba-Cu-O 2:4:7, the B_{3g} peaks appear at 314 or 305 cm^{-1} , and the B_{2g} peak at 228 or 236 cm^{-1} , respectively. Note that, contrary to the Y-Ba-Cu-O 1:2:4 spectrum in Fig. 4, there is no feature in the $y(xz)\bar{y}$ spectrum near 610 cm^{-1} .

We also took a spectrum (not shown) with the macroscopic Raman setup described in Sec. IV and found another peak in the xx spectrum near 108 cm^{-1} , which is somewhat higher than that of the corresponding peak in the Y-Ba-Cu-O 1:2:4 spectrum (Fig. 6).

VI. DISCUSSION

Frequencies, intensities and polarization selection rules of the peaks at 104 , 153 , 341 , 438 , and 500 cm^{-1} in Y-Ba-Cu-O 1:2:4 are very similar to those in the corresponding spectra in Y-Ba-Cu-O 1:2:3.² We argued in Sec. III that the Y-Ba-Cu-O 1:2:3 peaks are essentially unaffected by the introduction of a second Cu(1)-O(1) chain in Y-Ba-Cu-O 1:2:4. The immediate conclusion is that these peaks correspond, like in Y-Ba-Cu-O 1:2:3, to the A_g vibrations along the z axis of Ba (104 cm^{-1}), Cu(2) (153 cm^{-1}), O(2)-O(3) out-of-phase (341 cm^{-1}), O(2)-O(3) in-phase (438 cm^{-1}), and O(4) (500 cm^{-1}).

Using the same argument for Y-Ba-Cu-O 2:4:7, we can assign the observed peaks at 108, 147, 338, 448, and 500 cm^{-1} to the corresponding modes. We should repeat at this point that the intrinsic phonon frequencies of the Ba A_g mode are higher than the peak positions given here due to the strong Fano shape. We therefore should not place too much emphasis on the observed differences between Y-Ba-Cu-O 1:2:4, Y-Ba-Cu-O 2:4:7, and Y-Ba-Cu-O 1:2:3, the intrinsic frequencies might even be the same. The results are summarized in Table I.

It is interesting to note that the O(2)-O(3) in-phase phonon in Y-Ba-Cu-O 1:2:4 (438 cm^{-1} , similar to Y-Ba-Cu-O 1:2:3) is about 10 cm^{-1} lower than in Y-Ba-Cu-O 2:4:7, while the out-of-phase phonon seems to be harder. This observation cannot be explained by changes in atomic distances that are relatively small and would shift both phonons in the same direction. This yields additional evidence that simple bond-length considerations are not always adequate to describe phonon frequencies in high-temperature superconductors. Instead, it seems to be indispensable to consider directly the electronic structure which is probably very sensitive to doping, oxygen annealing, or ion replacement with valence changes even if the lattice parameters differ only marginally. In particular, the contribution of the chains to the Madelung energy, considerably asymmetric at the CuO_2 planes in the Y-Ba-Cu-O 2:4:7 compound, may be responsible for the observed frequency increase.

The spectra show two other A_g symmetry modes for Y-Ba-Cu-O 1:2:4 (Y-Ba-Cu-O 2:4:7) near 250 (250) and $605\text{ (606)}\text{ cm}^{-1}$. They are not due to impurity phases which would, most likely, not obey any polarization selection rules. Although the green phase Y_2BaCuO_5 has its strongest phonon near 605 cm^{-1} ,⁴¹ the observed peak cannot originate from it, since the second strongest phonon of that phase, around 390 cm^{-1} , is clearly missing. The group-theoretical analysis in Sec. III shows that vibrations of the Cu(1) and O(1) atoms along the z di-

rection are also Raman active in Y-Ba-Cu-O 1:2:4 and Y-Ba-Cu-O 2:4:7. We argued above that these peaks should be twice as large in Y-Ba-Cu-O 1:2:4 than in Y-Ba-Cu-O 2:4:7. This is indeed observed. We can therefore reliably assign the peaks at 250 and 605 cm^{-1} to the A_g phonons of Cu(1) and O(1), respectively. Also the frequencies are in agreement with the lattice dynamical discussion presented in Sec. III. The fact that the Cu frequency is rather high demonstrates that the double Cu(1)-O(1) chains are quite rigid.

Only the Cu(1), O(4), and O(1) phonons feel the a - b anisotropy, as is evident from the fact that they are present in yy but not in xx spectra. This stresses the important role of diagonal O(4)-O(1) and diagonal and y -oriented Cu(1)-O(1) bonds for the Raman activity of these modes. As expected, the chain phonons of Y-Ba-Cu-O 1:2:4 at 250 and 605 cm^{-1} are also in yy configuration about twice as large as in Y-Ba-Cu-O 2:4:7, which contains only half as many Raman-active double chains. But the behavior of the O(4) A_g phonon near 500 cm^{-1} is rather mysterious, since its yy component is in Y-Ba-Cu-O 1:2:4 much stronger than in untwinned Y-Ba-Cu-O 2:4:7 although the environment of the O(4) atom remains practically unchanged. This indicates that the polarizability of an O(4)-O(1) double-chain bond differs from that of an O(4)-O(1) single-chain bond. The fact that the Cu(2) phonon also shows in Y-Ba-Cu-O 1:2:4 a pronounced a - b anisotropy is surprising since Cu(2) is quite far away from the anisotropy-inducing chains. Furthermore, there exists practically no anisotropy in Y-Ba-Cu-O 2:4:7 (Figs. 7-9) or Y-Ba-Cu-O 1:2:3.³ This observation suggests that long-range Coulomb forces influence the Raman tensor of this mode.

According to the group-theoretical analysis, there should exist two B_{3g} and B_{2g} vibrations of O(1) and Cu(1) along the y and x axis, respectively, in Y-Ba-Cu-O 1:2:4 or Y-Ba-Cu-O 2:4:7 in addition to those in Y-Ba-Cu-O 1:2:3. Since no B_{2g} - B_{3g} modes have been convinc-

TABLE I. Frequencies (at 295 K), symmetries and assignments of the observed Raman phonons in Y-Ba-Cu-O 1:2:4, Y-Ba-Cu-O 2:4:7, and Y-Ba-Cu-O 1:2:3 (Ref. 3). NO stands for "not observed," a blank entry means that this phonon is not Raman active in Y-Ba-Cu-O 1:2:3. The given frequencies for Y-Ba-Cu-O 1:2:4 and Y-Ba-Cu-O 2:4:7 refer to the peak maxima in the spectra. For the Ba A_g mode, the intrinsic phonon frequency is higher (see text).

Symmetry	Assignment	Phonon frequency in cm^{-1}		
		Y-Ba-Cu-O 1:2:4	Y-Ba-Cu-O 2:4:7	Y-Ba-Cu-O 1:2:3
A_g	Ba	104	108	120
	Cu(2)	153	147	154
	Cu(1)	250	250	
	O(2)-O(3) out-of-phase	341	338	335
	O(2)-O(3) in-phase	438	448	435
	O(4)	500	500	500
	O(1)	605	606	
B_{2g}	Cu(1)	($\sim 140?$)	($\sim 140?$)	
	O(1)	228	236	
B_{3g}	Cu(1)	314	305	
	O(1)	NO	NO	

ingly observed in Y-Ba-Cu-O 1:2:3,²⁰ it is reasonable to assume that all observed B_{2g} - B_{3g} peaks correspond to chain vibrations. As discussed in Sec. III, the O(1) B_{3g} phonon should have a very high frequency (≈ 600 cm⁻¹), so the very strong B_{3g} symmetry peak at 314 cm⁻¹ in Y-Ba-Cu-O 1:2:4 observed in the $x(yz)\bar{x}$ spectrum must be due to the Cu(1) B_{3g} phonon. This rather high frequency again proves the stiffness of the double chains. In Y-Ba-Cu-O 1:2:4 this phonon is about twice as strong (relative to xx or yy spectra peaks) as in Y-Ba-Cu-O 2:4:7 (near 305 cm⁻¹), supporting its assignment as a double-chain-related mode. At this point, it remains unclear why the frequency is 9 cm⁻¹ lower in Y-Ba-Cu-O 2:4:7 although all double-chain Cu(1)-O(1) distances differ by no more than 0.5% between Y-Ba-Cu-O 1:2:4 and Y-Ba-Cu-O 2:4:7. In these materials, the O(1) B_{3g} mode as well as all other B_{3g} phonons seem to be too weak to be detectable.

The O(1) and Cu(1) atoms also perform vibrations along the x axis with B_{2g} symmetry. According to the calculations by Kress *et al.*³⁷ for single chain Y-Ba-Cu-O 1:2:3, they should have much lower frequencies (103 or 80 cm⁻¹, respectively) than the corresponding B_{3g} modes. We clearly observe one B_{2g} phonon near 228 cm⁻¹ in Y-Ba-Cu-O 1:2:4 and 236 cm⁻¹ in Y-Ba-Cu-O 2:4:7, again for Y-Ba-Cu-O 1:2:4 about twice as large as for Y-Ba-Cu-O 2:4:7, that can thus be assigned to O(1) B_{2g} vibration. Also for this phonon, the frequency difference between Y-Ba-Cu-O 1:2:4 and Y-Ba-Cu-O 2:4:7 cannot be explained by simple bond length considerations. The other peak in the $y(xz)\bar{y}$ spectrum near 140 cm⁻¹ might correspond to the Cu(1) B_{2g} phonons, but since the absence of this peak in all other spectra, and therefore its B_{2g} symmetry, cannot be proven, this assignment

remains tentative.

Finally, we discuss the appearance of a B_{2g} -like feature near 610 cm⁻¹ in the $y(xz)\bar{y}$ spectrum of Y-Ba-Cu-O 1:2:4, which does not show up in the Y-Ba-Cu-O 2:4:7 spectrum. We do not expect any chain mode in x direction with such a high energy. Also every Y-Ba-Cu-O 1:2:4 peak should also be observed in Y-Ba-Cu-O 2:4:7 spectra, as discussed in Sec. III. We therefore think that this peak is not due to an intrinsic B_{2g} mode, but possibly to some polarization leakage from the 605 cm⁻¹ A_g mode.

In conclusion, we have presented a complete Raman-phonon analysis of Y-Ba-Cu-O 1:2:4 and Y-Ba-Cu-O 2:4:7. We have observed and assigned four CuO chain phonons, including two strong phonons with B_{2g} and B_{3g} symmetry, respectively. We have compared the spectra for the two materials and shown that double-chain-related modes are twice as strong in Y-Ba-Cu-O 1:2:4, and that several phonon frequencies are shifted in a way that cannot be explained just by bond-length changes. One may conjecture that changes in the free carrier balance between planes and chains may account for these anomalies.

ACKNOWLEDGMENTS

The authors thank K. Peters for the determination of lattice parameters and crystal axes orientations and M. Gehrke for magnetic susceptibility measurements. H. Hirt, M. Siemers, and P. Wurster provided us with expert technical help. We acknowledge financial support from the Bundesminister für Forschung und Technologie, the European Community, and the Swiss Nationalfonds.

-
- ¹For a review, see C. Thomsen and M. Cardona, in *Physical Properties of High Temperature Superconductors*, edited by D.M. Ginsberg (World Scientific, Singapore, 1989), p. 409.
- ²For YBa₂Cu₃O₇, see R. Liu, C. Thomsen, W. Kress, M. Cardona, B. Gegenheimer, F.W. de Wette, J. Prade, A.D. Kulkarni, and U. Schröder, *Phys. Rev. B* **37**, 7971 (1988).
- ³C. Thomsen, M. Cardona, B. Gegenheimer, R. Liu, and A. Simon, *Phys. Rev. B* **37**, 9860 (1988).
- ⁴T. Ruf, C. Thomsen, R. Liu, and M. Cardona, *Phys. Rev. B* **38**, 11985 (1988).
- ⁵R. Hackl, W. Gläser, P. Müller, D. Einzel, and K. Andres, *Phys. Rev. B* **38**, 7133 (1988).
- ⁶F. Slakey, S.L. Cooper, M.V. Klein, J.P. Rice, and D.M. Ginsberg, *Phys. Rev. B* **39**, 2781 (1989).
- ⁷C. Thomsen, R. Liu, M. Bauer, A. Wittlin, L. Genzel, M. Cardona, E. Schönherr, W. Bauhofer, and W. König, *Solid State Commun.* **65**, 55 (1988).
- ⁸M. Hangyo, S. Nakashima, K. Mizoguchi, A. Fujii, A. Mitsuishi, and T. Yotsuya, *Solid State Commun.* **65**, 8 (1988).
- ⁹A.F. Goncharov, V.N. Denisov, J.P. Zibrov, B.N. Mavrin, V.B. Podobedov, Y.Ya. Shapiro, and S.M. Stishov, *Pis'ma Zh. Eksp. Teor. Fiz.* **48**, 453 (1989).
- ¹⁰E.T. Heyen, R. Liu, M. Garriga, B. Gegenheimer, C. Thomsen, and M. Cardona, *Phys. Rev. B* **41**, 830 (1990).
- ¹¹E.T. Heyen, R. Liu, B. Gegenheimer, C. Thomsen, M. Cardona, S. Piñol, and D. Mck. Paul, in *Phonons 89*, edited by S. Hunklinger, W. Ludwig, and G. Weiss (World Scientific, Singapore, 1990) p. 346.
- ¹²K.B. Lyons, P.A. Fleury, L.F. Schneemeyer, and J.V. Waszczak, *Phys. Rev. Lett.* **60**, 732 (1988).
- ¹³J. Karpinski, E. Kaldis, E. Jilek, S. Rusiecki, and B. Bucher, *Nature* **336**, 660 (1988).
- ¹⁴D.E. Morris, J.H. Nickel, J.Y.T. Wei, N.G. Asmar, J.S. Scott, U.M. Scheven, C.T. Hultgren, A.G. Markelz, J.E. Post, P.J. Heaney, D.R. Veblen, and R.M. Hazen, *Phys. Rev. B* **39**, 7347 (1989).
- ¹⁵P. Marsh, R.M. Fleming, M.L. Mandich, A.M. De Santolo, J. Kwo, M. Hong, and L.J. Martinez-Miranda, *Nature* **334**, 141 (1988).
- ¹⁶R.M. Hazen, L.W. Finger, and D.E. Morris, *Appl. Phys. Lett.* **54**, 1057 (1989).
- ¹⁷P. Bordet, C. Chaillot, J. Chenavas, J.L. Hodeau, M. Marezio, J. Karpinski, and E. Kaldis, *Nature* **334**, 596 (1988).
- ¹⁸D.E. Morris, N.G. Asmar, J.Y.T. Wei, J.H. Nickel, R.L. Sid, J.S. Scott, and J.E. Post, *Phys. Rev. B* **40**, 11406

- (1989).
- ¹⁹M.C. Krantz, H.J. Rosen, R.M. Macfarlane, N.G. Asmar, and D.E. Morris, *Physica C* **162-164**, 1089 (1989).
- ²⁰L.V. Gasparov, V.D. Kulakovski, O.V. Misochko, and V.B. Timoveev [*Physica C* **157**, 341 (1989)] reported the observation of B_{2g} and B_{3g} modes, which has not been confirmed by other groups. K.F. McCarty, J.Z. Liu, R.N. Shelton, and H.B. Radousky claim to have observed eight of the ten allowed B_{2g} and B_{3g} phonons [*Phys. Rev. B* **41**, 8792 (1990)].
- ²¹E.T. Heyen, R. Liu, M. Cardona, J. Karpinski, E. Kaldis, and S. Rusiecki (unpublished).
- ²²P. Fischer, J. Karpinski, E. Kaldis, E. Jilek, and S. Rusiecki, *Solid State Commun.* **69**, 531 (1989).
- ²³E. Kaldis, P. Fischer, A.W. Hewat, J. Karpinski, and S. Rusiecki, *Physica C* **159**, 668 (1989).
- ²⁴J. Karpinski, E. Kaldis, S. Rusiecki, E. Jilek, P. Fischer, P. Bordet, C. Chaillout, J. Chenavas, J.L. Hodeau, and M. Marezio, *J. Less Common Met.* **150**, 129 (1989).
- ²⁵J. Karpinski, S. Rusiecki, E. Kaldis, B. Bucher, and E. Jilek, *Physica C* **160**, 449 (1989).
- ²⁶P. Bordet, J.L. Hodeau, R. Argoud, J. Muller, M. Marezio, J.C. Martinez, J.J. Prejean, J. Karpinski, E. Kaldis, S. Rusiecki, and B. Bucher, *Physica C* **162-164**, 525 (1989).
- ²⁷J. Karpinski, C. Beeli, E. Kaldis, A. Wisard, and E. Jilek, *Physica C* **153-155**, 830 (1988).
- ²⁸J. Karpinski, S. Rusiecki, B. Bucher, E. Kaldis, and E. Jilek, *Physica C* **161**, 618 (1989).
- ²⁹C. Chaillout, P. Bordet, J. Chenavas, J.L. Hodeau, M. Marezio, J. Karpinski, E. Kaldis, and S. Rusiecki, *Solid State Commun.* **70**, 275 (1989).
- ³⁰A. Hewat, P. Fischer, E. Kaldis, J. Karpinski, and S. Rusiecki (unpublished).
- ³¹E. Kaldis and J. Karpinski, *J. Eur. Solid State Chem.* (to be published).
- ³²H.A. Ludwig, W.H. Fietz, M.R. Dietrich, H. Wühl, J. Karpinski, E. Kaldis, and S. Rusiecki, *Physica C* (to be published).
- ³³R.J. Wijngaarden and R. Griessen, in *Studies of High Temperature Superconductors*, edited by A.V. Narlikar (Nova Science, New York, 1988).
- ³⁴J. Schoenes, J. Karpinski, E. Kaldis, J. Keller, and P. de la Mora, *Physica C* **166**, 145 (1990).
- ³⁵M. Bauer (private communication); see also M. Bauer, I.B. Ferreira, L. Genzel, M. Cardona, P. Murugaraj, and J. Maier, *Solid State Commun.* **72**, 551 (1989).
- ³⁶D.L. Rousseau, R.P. Bauman, and S.P.S. Porto, *J. Raman Spectrosc.* **10**, 253 (1981).
- ³⁷W. Kress, U. Schröder, J. Prade, A.D. Kulkarni, and F.W. de Wette, *Phys. Rev. B* **38**, 2906 (1988).
- ³⁸W.E. Pickett, *Rev. Mod. Phys.* **61**, 433 (1989).
- ³⁹J.D. Jorgensen, M.A. Beno, D.G. Hinks, L. Soderholm, K.J. Volin, R.L. Hittermann, J.D. Grace, Ivan K. Schuller, C.U. Segre, K. Zhang, and M.S. Kleefisch, *Phys. Rev. B* **36**, 3608 (1987).
- ⁴⁰S.L. Cooper, M.V. Klein, B.G. Pazol, J.P. Rice, and D.M. Ginsberg, *Phys. Rev. B* **37**, 5920 (1988).
- ⁴¹Z.V. Popović, C. Thomsen, M. Cardona, R. Liu, G. Stanisić, and W. König, *Solid State Commun.* **66**, 43 (1988).